Development of a Virtual Sensor for State-of-Charge Evaluation of TCM-Energy Storage

Bernhard Zettl[1], Harald Kirchsteiger[1], Gayaneh Issayan[1], Waldemar Wagner[2], and Alois Resch[1]

[1] University of Applied Sciences Upper Austria (Austria)

[2] AEE- Institute for Sustainable Technologies (Austria)

Abstract

Sorption storage tanks for long-term heat storage have complex operating behavior that makes it difficult to determine the storage tank's state of charge. The approach of a virtual sensor is presented, which processes different measurement data and simulation data together in stages and thus helps to provide the process control with reliable and fail-safe data about the operating state of the memory.

Keywords: sorption storage, state of charge, zeolite, thermochemical energy storage, capacitive sensor

1. Introduction

Thermal energy storages (TES) are believed to be appropriate candidates to play an important role in the future thermal management system. Broad deployment of energy storage technologies for an increased share of renewable energy is motivated by global climate action and the ambition of CO2 reduction.

The ability of thermochemical materials (TCM) to store energy long-term with practically no losses during the conservation phase makes them promising candidates for seasonal storage applications. High energy densities using the zeolite-water couple have been demonstrated for some applications, exceeding those of water storage by a factor of 2-3 (Hauer, 2020) (Zettl, 2020). There are several process solutions for sorption technology, open and closed systems, as well as moving-bed and fixed-bed reactions, which have specific advantages.

For all types of energy storage, the current state of charge (SOC) is an important parameter for operation and control. In contrast to sensible heat storage, the state of charge of thermochemical storage cannot be determined via the current discharge temperature. Rather, the current moisture content of the material and the moisture distribution over the entire storage system is a representative value for the state of charge. Since the material moisture balance is much more difficult to measure with “inline” methods (without taking probes) than the temperature, various physical measurement methods were tested in a preliminary project. One of the best ways is to utilize the dielectric conductivity, or permittivity, which correlates with the moisture content of the material. It can be detected, for example, by utilizing microwaves or by determining electrical capacitance (Zettl, 2022). However, the moisture measurement methods react sensitively to density fluctuations and temperature differences in the material, therefore comprehensive error correction and the combination of different measurement methods can improve accuracy here. For this purpose, a virtual sensor is being developed that eliminates various factors that interfere with the measurement and significantly increases the measurement quality.

2. Methodology

2.1 Sensor architecture

There are currently no sensors available for directly measuring the state of charge of sorption materials storage systems. An indirect method relying on electrical capacitance measurement was shown to be feasible in a laboratory environment (Kirchsteiger and Kefer, 2020). However, the method suffers from calibration requirements which potentially restrict practical applications: Material density fluctuations in moving bed applications and temperature influences the signals widely. SOC determination can be significantly enhanced by combining hardware sensors with appropriate mathematical models for so-called virtual sensors.

doi:10.18086/eurosun.2022.13.24 Available at http://proceedings.ises.org

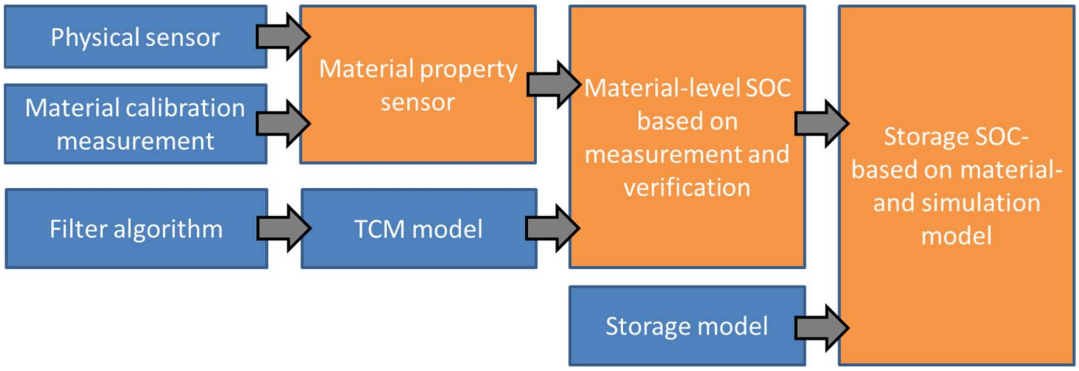

Fig. 1: Principle of the operating levels of the virtual sensor

From a systems-theory point of view, the SOC of the sorption storage is an internal state which is not accessible for direct measurement (orange elements in Fig.1). There is the possibility to estimate this internal state using sophisticated software tools such as dynamic state observers. A particular type of observer, known as Kalman-filter, is implemented to take advantage of a combined model-based and real-time measurement strategy. Appropriately tuned, the filter assures a balanced SOC estimate which is not directly affected by short-time measurement errors (for example: temporary drops in a temperature measurement) since they are not plausible compared to the implemented model. At the same time, inevitable systematic model deviations are compensated with the aid of real-time measurements.

2.2 Adsorption model

The material adsorption model used in this work represents a sorption storage system of a zeolite bed. An axial humid airflow or vapor diffusion drives the sorption process and allows direct charging/discharging of the sorption material. The model implementation is done in Simulink, an additional package of MATLAB. To perform the numerical simulations, the model is based on the following assumptions (Daborer-Prado, et al., 2019):

- a one-dimensional approach is assumed, where no radial influence is considered
- a lumped element storage model is used for material and airflow, it is assumed that the air leaves each store node with the node temperature
- the sorption equilibrium is modelled by the Dubinin-Astakhov-approach and the reaction kinetics is described by a linear driving force approach
- the specific heat capacity of the air is not a function of the humidity or the temperature in the system; the specific heat capacity of the solid is only a function of humidity (water loading) but not of the temperature in the system.

2.3 System simulation

The system simulation is based on the specific procedural features of the open and closed sorption systems, which differ in their boundary conditions. The principle of operation of typical reactor elements is shown in Fig. 2. These elements can be enlarged and combined into a more complex system to represent the storage system. Specific operating situations such as partial loading, diffusion, external losses, and internal leveling processes within the system and material changes (degradation) must be represented separately from the typical cells.

The SOC determination on the three levels, material properties, local SOC, and system SOC is intended to largely rule out errors:

- The material calibration procedure determines the relationship between the physical sensor signal and material properties
- The filter algorithm and the adsorption model verify the material property changes based on the process parameters and determine the (local) material loading,
- The storage simulation model considers the process technology and operational management of the entire

system (the sum of all cells and boundary conditions)

Using this step-by-step approach and with the help of an experimental setup and measured data for training and demonstrating the virtual sensor operation, a sophisticated approach to SOC determination for thermochemical storage is developed and a reliable metric for process control is developed.

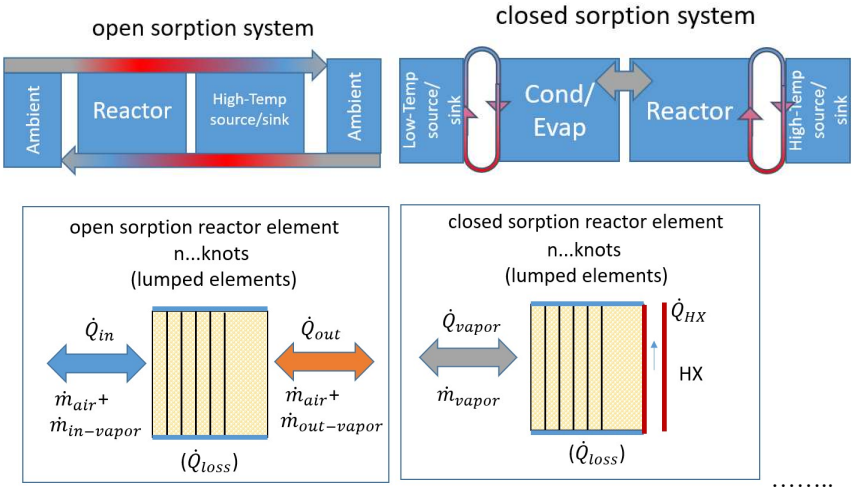

Fig. 2: Operating principle of the closed and open sorption TES (above) and the boundary conditions of two typical reactor elements

3. Experimental Results

3.1. Open Sorption Reactor

In an open moving bed reactor, a capacitive sensor is used between which electrodes the material is allowed to move freely (Fig. 3). Depending on the moisture content of the material, the electrical permittivity changes and with it the effective capacitance value of the capacitor.

To record the signal, the capacitor is integrated into a parallel resonant circuit and the resonant frequency of the resonant circuit is reacting on the moisture content of the material. The resonant frequency is therefore used as a relatively sensitive but stable indicator of the material moisture. The resonant frequency of the oscillating circuit is around 196 kHz, the capacitance of the unfilled capacitor 8.8 pF. A turntable with a diameter of 100 cm and a material volume of 15 litres simulates the moving bed of a storage system. The rotating speed of the disk is about 5 revolutions per minute.

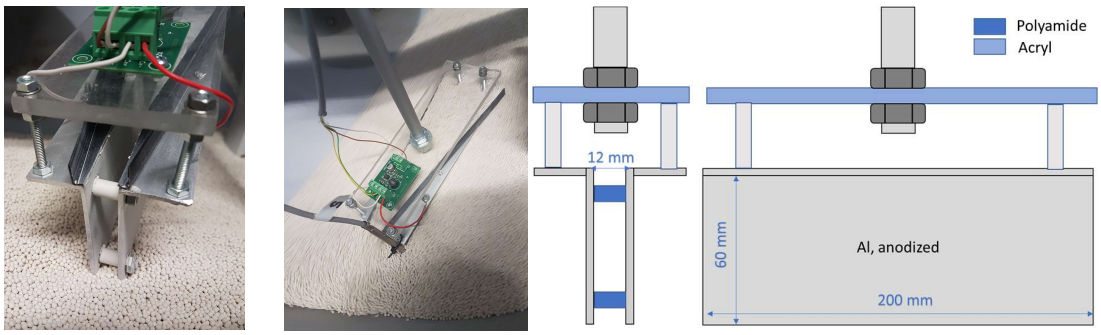

Fig. 3: Parallel plate capacitor placed in a moving bed of zeolite granules of 1.5-2.5mm diameter.

The dehydrated zeolite (12h @ 250°C) is filled into the turntable and ventilated with moist air from an ultrasonic fogger. Samples are taken at periodic intervals and the material moisture is measured using the reference measurement (2 hours in a drying furnace @ 350°C). The measurement ends when no further moisture increase is recognized in the zeolite bed. The material moisture content achieved in the experiment is approx. 5-10% lower compared to the manufacturer's data sheet.
The measurement result for two types of zeolite in four different varieties is shown in the figures below.

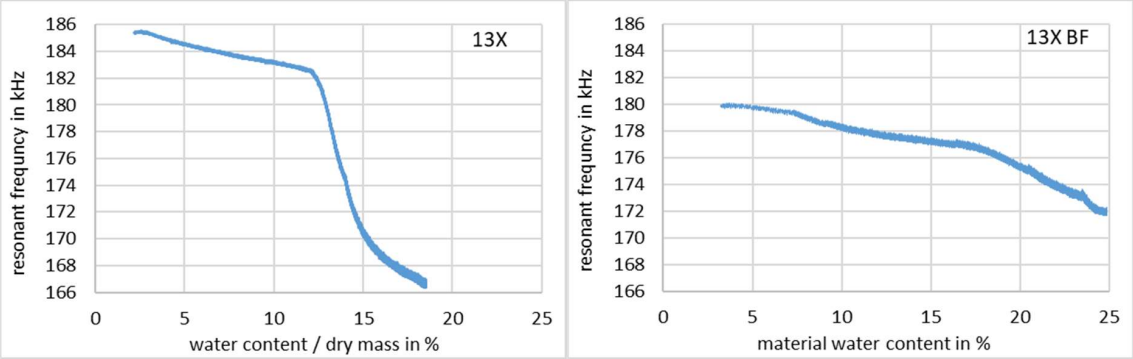

Fig. 4: Measured resonant frequency during the adsorption experiment at low temperature (25-40°C) in zeolite 13X (left) and 13X binder free (right), both 1.5-2.5 mm granules.

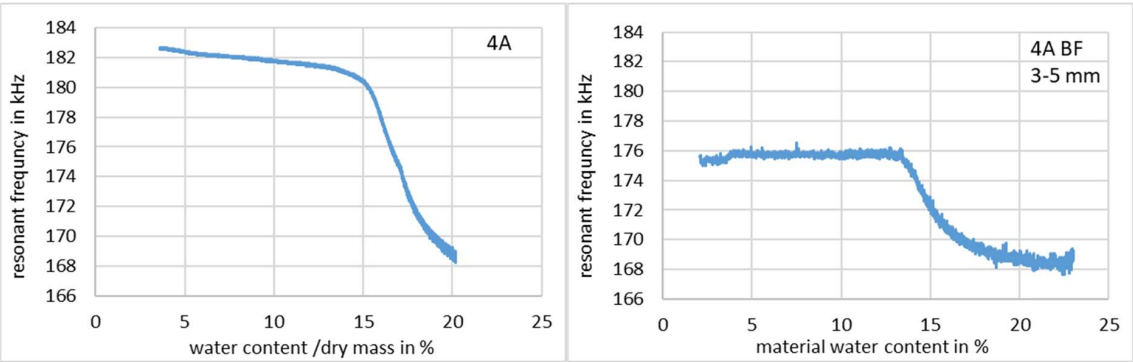

Fig. 5: Measured resonant frequency during the adsorption experiment at low temperature (25-40°C) in zeolite 4A 1.5-2.5 mm granules (left) and 4A binder free, 3-5 mm granules (right).

The results of the experiments show a clear influence of the material humidity on the resonant frequency. In general, the higher the humidity the lower the resonant frequency, but influence is non-linear: rate of frequency drop at the beginning of the experiment (dry material) is lower, for more humid material frequency drop is higher. For 4A-BF, no frequency change until approx. 13 wt.% of water was detected.

The temperature also plays a certain role, in general, higher temperatures tend to lower the resonant frequency. For adsorption reactions in the range of 30-50°C, the temperature plays no important role for zeolite 13X since the humidity influence is dominant. For other zeolites such as 4A-BF further calibration measurements should lead to a kind of temperature correction term for the resonant frequency. For high temperature desorption application (150-250°C) of the suggested measurement principle, separate calibration measurement would be necessary.

As mentioned earlier the resonant frequency relies on the active capacity in the electronic oscillator, while the capacity value itself consist of the addition of several parts: the electronic capacity inside the electronic circuit (C_p), the capacity of the sensor cable (C_C), and the sensor itself including the material (C_s). The built-in components of the oscillator are: C_p=470 pF and L=1.4 mH, the oscillator-print itself (without external components) exhibit an resonance frequency of 196.11 kHz.

$$f_r = \frac{1}{2\pi\sqrt{LC}} \quad ....resonant\ frequnecy \qquad \text{(eq. 1)}$$

$$C = C_p + C_c + C_s \,....capacity \qquad \text{(eq. 2)}$$

$$C_s = \varepsilon\frac{A}{d}, \quad \varepsilon = \varepsilon_r\varepsilon_0, \quad \varepsilon_0 = 8{,}845\ 10^{-12} As/Vm \qquad \text{(eq. 3)}$$

A certain drop of the resonant frequency indicates an increase of the sensor capacity C_s, according to eq.1 and 2 due to an increase of relative permittivity ε_r according to eq.3. After connecting sensor and cable to the oscillator resonance frequency decreases by 3.3 kHz, which corresponds to an additional capacity C_c+C_s= 16.5 pF while C_s= 8,9 pF (according to eq.3). By measuring the further frequency decrease after inserting into the zeolite bed the permittivity of the material while humidified can be calculated.

$$\varepsilon_r = \frac{1}{\varepsilon_0}\frac{d}{A}\left(\frac{1}{L}\left(\frac{1}{2\pi f_r}\right)^2 - C_p - C_c\right) \qquad \text{(eq. 4)}$$

Calculating the relative permittivity out of the recorded frequencies leads to the results shown in Fig.6. The permittivity of the dry zeolite is in the range of ε_r =5….10, while in the hydrated material ε_r rises to 15…20. For comparison, dielectric properties of various minerals can be found in the literature. The values for sand or clay with a material moisture content between 0…..20% are comparable, with measured values of ε_r in the range of 5 to 20.

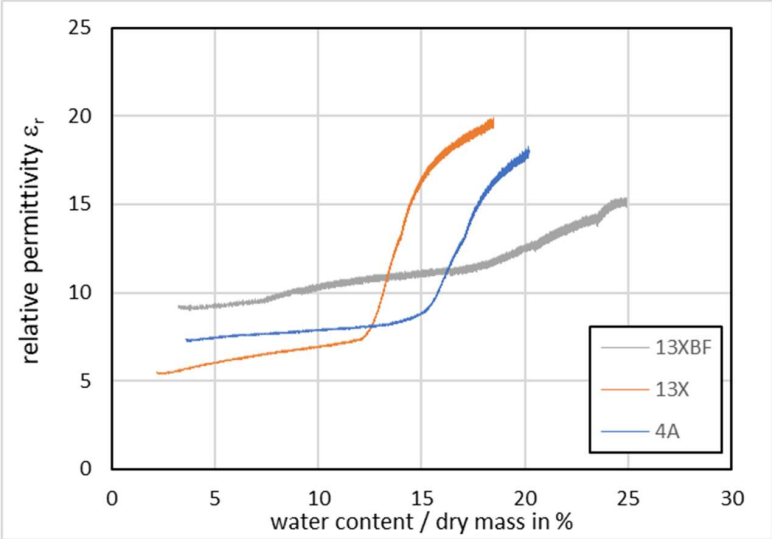

Fig. 6: Calculated relative permittivity of different zeolites

In literature the development of the dielectric constant is explained with the help of a multiphase model. In porous minerals and soils, water fraction below the point WP (Fig. 7) are addressed as “bound water”, above the porosity point P as “free water” and between as “mixed state”, producing a multi-phase signal (Park, C.-H., et.al., 2017). The so-called wilting point WP refers to a certain water fraction in a hydroscopic porous material, below which water is bound by adsorption (e.g., in clay and soil, plants are not able to benefit from it). In adsorption process engineering, the multiphase model refers to the formation of layers of adsorbate in the pores of the adsorbent: the first layer is bound more strongly than the second and subsequent ones, which form capillary condensation.

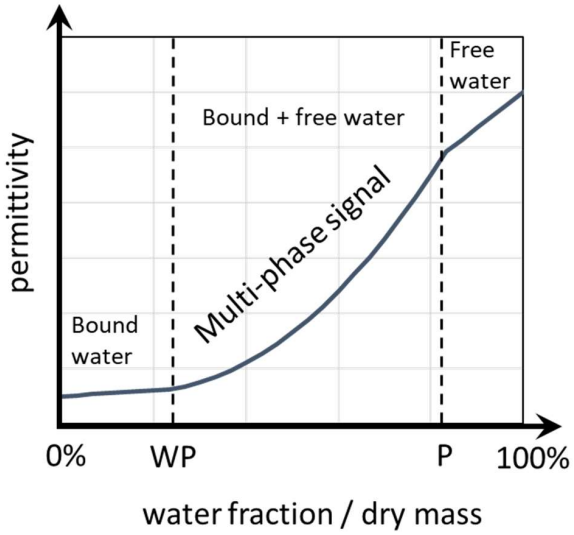

Fig. 7: Multiphase model of dielectric constant (permittivity) of humid minerals, redrawn from (Park, C.-H., et.al., 2017)

3.1. Closed Sorption Reactor

For the application in a closed sorption vessel, there are several challenges for the sensor technology, such as vacuum resistance, resistance to high temperatures (up to 200°C) during desorption, the influence of the measurement signal by the fixed-bed heat exchanger and by the locally different reaction states in the storage tank.

As shown in Fig. 8, a sector cylinder condenser was developed, which contains in the inside the same sorption material as the rest of the storage tank. The water uptake of the internal sorption material inside the enclosure

influences the capacitor and the measurement, therefore. Due to the large dimension of closed sorption vessels several regions are covered by linked sectors of the cylindrical capacitor.Fig. Fig. 9 shows a picture of several coupled sectors, so that several areas in the fixed-bed storage tank can be measured simultaneously with one sensor installation.

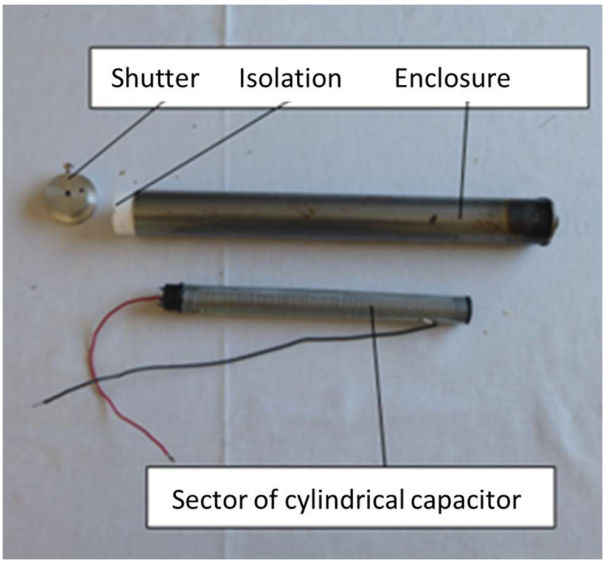

Fig. 8: Setup of the cylinder condenser

Fig. 9: Coupling of several sector cylinder condensers

Fig. 10 shows the characteristic frequency curves of the zeolite 13X BF as a function of the temperature and the degree of humidity in a fixed bet reactor. They act as the basis for programming a microprocessor when the measured frequencies and temperatures are interpreted as the degree of humidity in the measured sector.

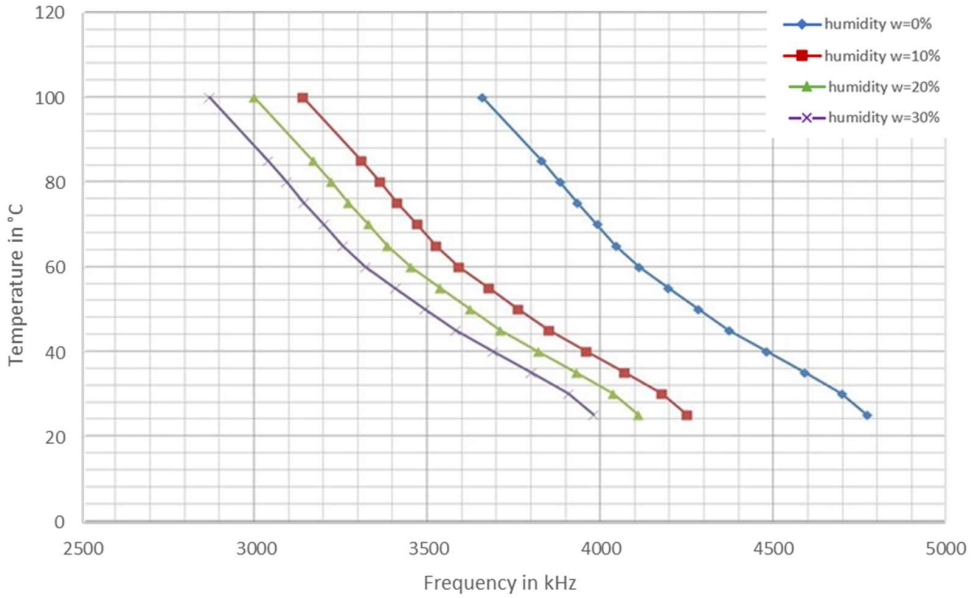

Fig. 10: Characteristic frequencies of zeolite 13X BF as a function of the temperature and the degree of humidity

The measurement results obtained by using an oscillator in the 2.5-5.0 GHz frequency range clearly show the combined humidity and temperature influence and are usable for calibration of the data controller, therefore.

4. Filter Development

4.1. General Function of Kalman Filter

A Kalman Filter is a virtual dynamical system (a computer algorithm) which is generating an estimate $\hat{x}$ of the current state x of a real dynamical system based on the history of input (u) and output (y) measurement data from the real system and a mathematical model of the system (Grewal and Andrews 2001). There are numerous applications of Kalman filters as real-time estimators, for example SOC and state of health estimation in battery cells, estimation of position and orientation of moving objects such as quadcopters for example, based on easily available accelerometer measurements. In general, it enables to estimate an internal quantity of a process which is otherwise not accessible through direct measurement, hence the alias "virtual sensor". Since the filter works with real-time measurement data, its results are affected by the corresponding measurement noise. However, under certain statistical assumptions (Simon 2006) it can be guaranteed that the Kalman Filter is a mathematically optimal estimator for linear systems in the sense that the covariance of the state estimation error is minimized.

4.2. Adsorption Model Adaption

The concept of the Kalman Filter is applied to the problem of determining the current state of charge of a sorption storage system. Here, we are considering a fixed-bed sorption storage using zeolite as sorption material as it was presented and mathematically modelled in Daborer-Prado, N., et.al. (2020). This model forms the basis for the model development required for the Kalman Filter. We are considering the 1-node model (the entire longitudinal direction of the storage is considered as one element with one lumped parameter for the water load) which uses as internal states to describe the dynamics

$$x = [x_s \quad x_G \quad T_s \quad T_{brd}]^T \qquad \text{(eq. 5)}$$

where x_s is the water load of the sorptive material, x_G is the water load of the gas flowing through the storage, T_s is the temperature of the sorptive material, and T_{brd} is the temperature on the storage exterior. The model inputs are

$$u = [m_G^{IN} \quad x_G^{IN} \quad T_G^{IN}]^T \qquad \text{(eq. 6)}$$

where m_G^{IN} is the mass flow of the gas through the storage, x_G^{IN} is the absolute humidity of the gas flow with respect to dry air, and T_G^{IN} is the temperature of the inflow gas. For details of the model development, we refer to the paper Daborer-Prado, N., et.al. (2020). The mathematical model to be used in the design phase of the Kalman Filter differs from the described simulation model. One central difference is the way how the water load x_G is treated: in the simulation model a spatial differential equation describes its behaviour with respect to the longitudinal direction, while temporal differential equations describe the outcome of the outflow water load x_G^{OUT} at the point where gas leaves the storage, depending on the other state variables x. A standard Kalman Filter requires a system of ordinary differential equations, therefore model adaptations were made in the following way.

A data-driven state space model of second order was developed which approximatively provides the quantity x_G^{OUT} as output and uses the quantities (x_s, T_S) as input. To estimate this model, data sequences at various stationary choices of the inputs u were generated using the simulation model. The estimated model obtained fit-values (a measure of the coincidence of model output and data sequences) of more than 90% on all datasets. This model contains two new state variables x_1 and x_2. The overall mathematical model for the Kalman Filter combines those two states with the ones from the simulation model described above to the augmented state vector

$$x_{KF} = [x_s \quad x_1 \quad x_2 \quad T_S \quad T_{brd}]^T \qquad \text{(eq. 7)}$$

Further assumptions were made in the development process of the Kalman Filter

- The input x_G^{IN} was assumed to be constant throughout an experiment
- The input T_G^{IN} was assumed to be constant throughout an experiment
- The states T_S and T_{brd} are assumed to be accessible through measurement on the device

Altogether, the mathematical model can be described in the general form of a continuous time nonlinear state-space model with the state x_{KF} and the input m_G^{IN}:

$$\dot{x}_{KF} = f(x_{KF}, m_G^{IN}) \quad \text{(eq. 8)}$$

As a next step, the model needs to be transferred into discrete-time. For this purpose, a simple Euler approximation with a sample time ΔT is utilized and given in the general formulation:

$$x_{k+1} = x_k + \Delta T\, f(x_k, u_k) \quad \text{(eq. 9)}$$

Note that this model is non-linear since the dynamics of the original simulation model are also nonlinear. Therefore, a standard linear Kalman Filter is not applicable and the extension of an extended Kalman Filter (EKF), see e.g. (Grewal and Andrews 2001) capable of dealing with nonlinearities could be used instead. A natural approach would also be to linearize the model around one stationary operating point and assume "small" deviations from this point during operation. There is, however, no stationary operating point in the considered application since the load x_s will continue to rise (in adsorption mode) even if all the input quantities are fixed to constant values inside the operating conditions. Therefore, an EKF was developed and implemented in the MATLAB® /Simulink™ environment using the built-in EKF functionality. The general overview of the system can be seen in Figure 11.

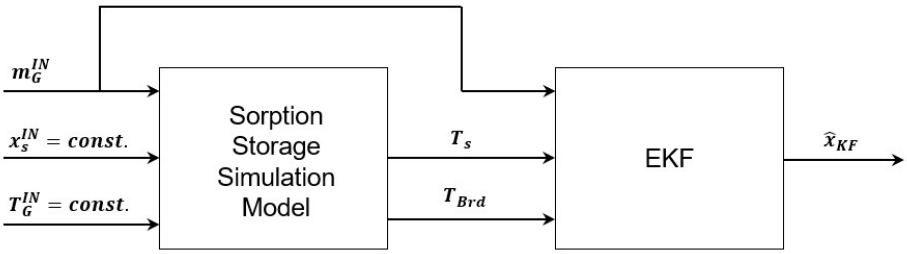

Fig. 11: Overview of the MATLAB® /Simulink™ simulation model

To demonstrate the quality of the state estimation, a simulation where the input was chosen to $m_G^{IN} = 300$ kg/h and the sorption material had an initial humidity of $x_s(t = 0) = 0.1$ was performed. The results are graphically shown in Figure 12, where the blue lines represent the quantities derived from the simulation model and the red lines are the state estimates from the EKF. Since the initialization of the EKF does not match precisely the initial conditions of the simulation model (which is a realistic assumption), there are minor deviations between the two lines in the beginning of the experiment. This is an expected behaviour of virtually any Kalman Filter application unless initial states are perfectly known. As the experiment continues, the lines begin to coincide, especially the two temperatures shown in the bottom two panels. This is because those temperatures are directly measured and the tuning of the EKF was done in such a way that the errors introduced in those measurements are assumed to be small in comparison to the errors introduced in the modelling of the states x_S and x_G. In other words, the measurement covariance was chosen much smaller than the covariance of the additive process noise affecting the model states. With respect to the actual variable of interest, the water load x_S, shown in the top panel, the EKF can reproduce its trajectory in a sufficient way and only introduces a minor offset.

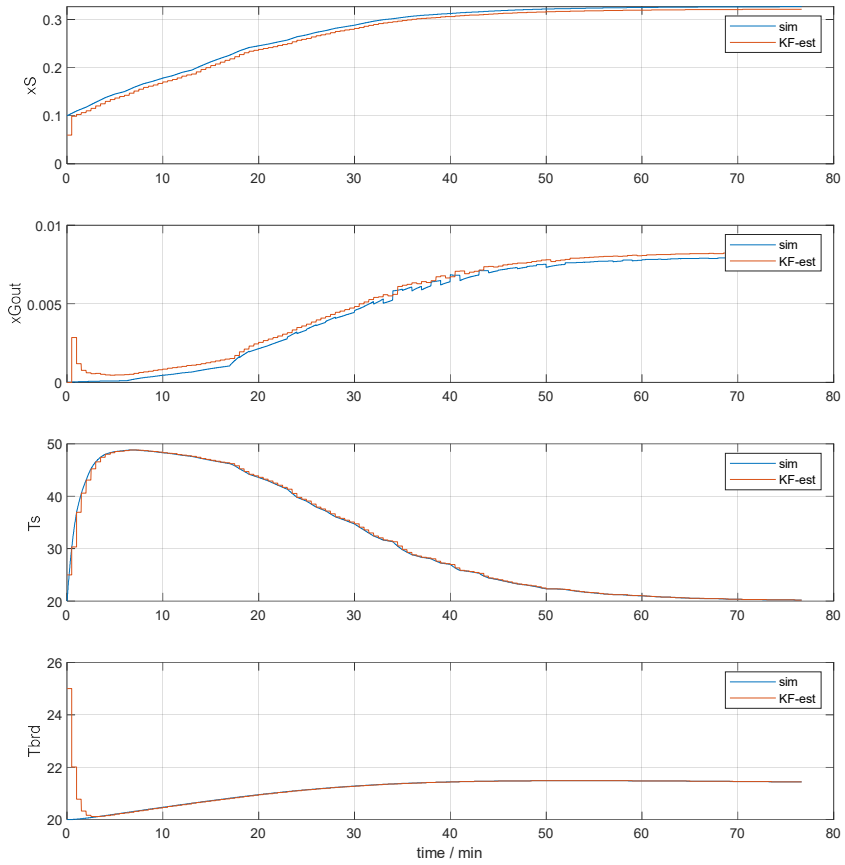

Fig. 12: Comparison of the EKF-estimated states with the simulation model

5. Summary

In order to develop a new State-of-Charge (SOC) sensor, the concept of a virtual sensor concept was applied, combining physical measurements, adsorption model, and system simulation.

- Calibration data is used to exhibit the material relative permittivity dependence to the material humidity.
- In the 200 kHz frequency range, material water content is the dominant factor that influences the relative permittivity of 13X-BF zeolite, other materials like zeolite 4A show little changes likewise.
- In the 2 MHz frequency range, a pronounced influence of both, temperature and humidity was measured.
- The Kalman-filter is suitable to repress sensor failures by estimating the material characteristics based on a modified adsorption model. The model allows the fast in-line prediction of the future material humidity load based on the current state, sensor signals and the modified adsorption model.
- A system simulation will be used to integrate the virtual sensor into a SOC determination of the entire storage system.

6. Acknowledgments

The work was carried out in the project “SorSens”, financially supported by the Austrian Climate and Energy Fund (KLIEN) and the Austrian Research Fund (FFG-grant number 881187). Ext. Projektnummer: WI-2020-701794/12-Cz and the project RESINET, funded in the framework if IWB Investitionen in Wachstum und Beschäftigung 2014 – 2020, Upper Austria. Furthermore, the work was supported by the research project “Heat Highway” (reference number 880797, funding program “Vorzeigeregion Energie”), co-financed by the “Klima- und Energiefonds” and the government of Upper Austria.

7. References

Daborer-Prado, N., Kirchsteiger, H., Zettl, B., Asenbeck, S., Kerskes, H., 2020. Mathematical modeling of rotating sorption heat storages. Proceedings of the ISES Solar World Congress 2019 and IEA SHC International Conference on Solar Heating and Cooling for Buildings and Industry 2019. DOI: http://dx.doi.org/10.18086/swc.2019.22.01

Grewal, M.S., Andrews, A.P., 2001. Kalman Filtering: Theory and Practice, 2nd edition, John Wiley & Sons, 2001. DOI: http://dx.doi.org/10.1002/9780470377819

Hauer, A., Fumey, B., Gschwander, S., Lager, D., Lázaro, A., Rathgeber, C., Ristić, A., van Helden, W., Issayan, G. Zettl, B., 2020. Material and Component Development for Thermal Energy Storage. IEA SHC Task 58 / ECES Annex 33 IEA ECES Annex 33 - Final Report, p. 82 – 86.

Issayan, G., Zettl, B., 2021. Processing Salt-Hydrates to Thermochemical Storage Composite Materials. 15th International Virtual Conference on Energy Storage ENERSTOCK, Book of Abstracts. p. 95 – 96

Issayan, G., Zettl, B., Somitsch, W., 2021. Developing and Stabilizing Salthydrate Composites as Thermal Storage Materials. 14th International Renewable Energy Storage Conference 2020 (IRES2020) AtlantisPress, p.49-57. DOI: http://dx.doi.org/10.2991/ahe.k.210202.008

Issayan, G., Zettl, B., 2022. Novel Thermogravimetric Characterization Method for Adsorption Cycles of TCM. 15th International Renewable Energy Storage Conference 2021 (IRES2021) AtlantisPress, p.108-117. DOI: http://dx.doi.org/10.2991/ahe.k.220301.011

Kirchsteiger, H. and Kefer, P. “A Novel State of Charge Sensor Concept for Thermochemical Heat Storage.” 13th international conference on solar energy for buildings and industry (EUROSUN 2020), Athens, Greece, 2020. DOI: http://dx.doi.org/10.18086/eurosun.2020.07.09

Jin, X., Yang, W., Gao, X., Li, Z., 2020. Analysis and Modeling of the Complex Dielectric Constant of Bound Water with Application in Soil Microwave Remote Sensing, Remote Sens. 12 (2020), pp 3544, DOI: http://dx.doi.org/10.3390/rs12213544

Park, C.-H., Behrendt, A., LeDrew, E., Wulfmeyer, V., 2017. New Approach for Calculating the Effective Dielectric Constant of the Moist Soil for Microwaves, Remote Sens. 9 (2017) pp 732. DOI: http://dx.doi.org/10.3390/rs9070732

Simon, D. 2006. Optimal State Estimation: Kalman, H∞, and nonlinear Approaches. John Wiley & Sons, 2006. DOI: http://dx.doi.org/10.1002/0470045345

Zettl, B., 2020. Long-term thermochemical heat storage for low temperature applications. Proceedings of the ISES Solar World Congress 2019, p. 397-402. DOI: http://dx.doi.org/10.18086/swc.2019.08.11

Zettl, B., 2022. State-of-Charge measurement techniques for PCM and TCM IEA SHC T67/ ECES Annex 40, 2nd Expert Meeting Graz, 2-4 April 2022. DOI: http://dx.doi.org/10.1016/j.egypro.2016.06.205